

1990

Hamiltonian Chaos

Niraj Srivastava
University of Rhode Island

Charles Kaufman
University of Rhode Island, chuck@uri.edu

Gerhard Müller
University of Rhode Island, gmuller@uri.edu

Follow this and additional works at: https://digitalcommons.uri.edu/phys_facpubs

Citation/Publisher Attribution

N. Srivastava, C. Kaufman and G. Müller. *Hamiltonian chaos*. *Computers in Physics* 4 (1990), 549-553.
Available at: <http://dx.doi.org/10.1063/1.4822945>

This Article is brought to you by the University of Rhode Island. It has been accepted for inclusion in Physics Faculty Publications by an authorized administrator of DigitalCommons@URI. For more information, please contact digitalcommons-group@uri.edu. For permission to reuse copyrighted content, contact the author directly.

Hamiltonian Chaos

Publisher Statement

Copyright 1990 American Institute of Physics. This article may be downloaded for personal use only. Any other use requires prior permission of the author and the American Institute of Physics.

The following article appeared in Computers in Physics and may be found at <http://dx.doi.org/10.1063/1.4822945>.

Terms of Use

All rights reserved under copyright.

Hamiltonian Chaos

Niraj Srivastava, Charles Kaufman, and Gerhard Müller

Department of Physics, University of Rhode Island, Kingston, RI 02881-0817.

Cartesian coordinates, generalized coordinates, canonical coordinates, and, if you can solve the problem, action-angle coordinates. That is not a sentence, but it is classical mechanics in a nutshell. You did mechanics in Cartesian coordinates in introductory physics, probably learned generalized coordinates in your junior year, went on to graduate school to hear about canonical coordinates, and were shown how to solve a Hamiltonian problem by finding the action-angle coordinates. Perhaps you saw the action-angle coordinates exhibited for the harmonic oscillator, and were left with the impression that you (or somebody) could find them for any problem. Well, you now do not have to feel badly if you cannot find them. They probably do not exist!

Laplace said, standing on Newton's shoulders, "Tell me the force and where we are, and I will predict the future!" That claim translates into an important theorem about differential equations—the uniqueness of solutions for given initial conditions. It turned out to be an elusive claim, but it was not until more than 150 years after Laplace that this elusiveness was fully appreciated.

In fact, we are still in the process of learning to concede that the proven existence of a solution does not guarantee that we can actually determine that solution. In other words, deterministic time evolution does not guarantee predictability. Deterministic unpredictability or *deterministic randomness* is the essence of chaos. Mechanical systems whose equations of motion show symptoms of this disease are termed *nonintegrable*. Nonintegrability is not the result of insufficient brainpower or inadequate computational power. It is an intrinsic property of most nonlinear differential equations with three or more variables.

In principle, Newton's laws can predict the indefinite future of a mechanical system. But the distant future of a nonintegrable system must be "discovered" by numerical integration, one time step after another. The further into the future that prediction is to be made, or the more precise it is to be, the more precise must be our knowledge of the initial conditions, and the more precise must be the numerical integration procedure. For chaotic systems the necessary precision (for example, the number of digits to be retained) increases exponentially with time. The practical limit that this precision imposes on predictions made by real, necessarily finite, computation was emphasized in a recent article in this column.¹

In the Hamiltonian formulation of classical dynamics, a system is described by a pair of first-order ordinary differential equations for each degree of freedom i . The dynamical variables are a canonical coordinate q_i and its conjugate

momentum p_i for each degree of freedom. For a particle of mass m moving along the x -axis and subject to a force $F(x) = -dV(x)/dx$, the position x and the momentum $p = m\dot{x}$ are a pair of canonically conjugate variables. The same particle moving in three-dimensional Euclidean space and subject to the force $\vec{F}(\vec{r}) = -\vec{\nabla}V(\vec{r})$ represents a system with three degrees of freedom, describable in terms of three pairs of canonical coordinates (x, p_x) , (y, p_y) , (z, p_z) . For such non-constrained mechanical systems, the Hamiltonian is simply the total energy expressed in these variables, $H = (p_x^2 + p_y^2 + p_z^2)/2m + V(x, y, z)$. In many mechanical systems the Cartesian coordinates are subject to constraints and, as we will see, the canonical coordinates q_i, p_i must then be determined by a more complicated procedure.

For any given Hamiltonian $H(q_1, \dots, q_N, p_1, \dots, p_N)$, the time evolution of the canonical coordinates is determined by the $2N$ canonical equations

$$\dot{q}_i = \frac{\partial H}{\partial p_i} \quad \text{and} \quad \dot{p}_i = -\frac{\partial H}{\partial q_i}, \quad i = 1, \dots, N. \quad (1)$$

The canonical coordinates might not be the most suitable set of variables in which to numerically integrate a dynamical system. If a noncanonical set is used, the canonical coordinates should be monitored to analyze the underlying physics.

The canonical coordinates of a dynamical system with N degrees of freedom span a $2N$ -dimensional space called the *phase space* of the system. A state of the system is specified by a single point in that space. As the system evolves in time, the point traces out a *trajectory* in phase space. These trajectories have two general properties that are important for our discussion. They cannot intersect each other or themselves, a direct geometrical implication of the uniqueness theorem mentioned previously. For autonomous Hamiltonian systems, the Liouville theorem further implies that a volume element in phase space cannot become smaller or larger as the points within it evolve in time. The flow of phase points resembles that of an incompressible fluid. There are no attractors, strange or otherwise. Hamiltonian chaos must have a different signature.

First consider a system with one degree of freedom, specified by a Hamiltonian $H(q, p)$ representing the conserved energy of the system. The equation, $H(q, p) = \text{const}$, completely determines the trajectory in (q, p) -space. For bounded motion, all trajectories are closed, and the motion along any trajectory is periodic in time. (The period diverges for special trajectories, located on *separatrices*.) There is no room for chaos in $2d$ phase space.

Now consider a system with two degrees of freedom, specified by the Hamiltonian $H(q_1, q_2, p_1, p_2)$. In this case the single equation $H = \text{const}$ does not determine the course of a trajectory in $4d$ phase space, but imposes a much weaker constraint. It defines a $3d$ hypersurface in $4d$ phase space on which all trajectories for a given energy are confined. If this constraint is the only one, the trajectories can easily avoid themselves or each other, and the nonintersection requirement does not restrict the degree of possible complexity of individual trajectories.

The existence of a second independent conserved quantity, $I(q_1, q_2, p_1, p_2)$, specifies another $3d$ hypersurface that is invariant under time evolution. I is referred to as an *integral of the motion* or *analytic invariant*. Any given trajectory lies on the intersection of the two surfaces specified by $H = \text{const}$ and $I = \text{const}$, a $2d$ surface in $4d$ space. It is less obvious to show but important for our discussion that this surface has the topology of a torus (the *invariant torus*).² Since it is difficult to visualize objects in $4d$ space, even $2d$ objects, we wish to look at the invariant torus as it appears on the $3d$ energy hypersurface where it has the shape of a doughnut. The entire energy hypersurface is densely foliated by such doughnuts and the entire phase space by invariant tori.

The existence of a second integral of the motion I implies the existence of a special *canonical transformation* from the canonical coordinates q_1, q_2, p_1, p_2 to the action-angle coordinates J_1, J_2, ϕ_1, ϕ_2 . In (q_1, q_2, p_1, p_2) -space, the local J_i -axes are perpendicular to and the local ϕ_i -axes tangential to any given invariant torus. The torus is then specified by the (time-independent) action coordinates J_1, J_2 alone, and the motion of the phase point on the torus by the angle coordinates $\phi_1(t), \phi_2(t)$.

Since the torus lies entirely on a given energy hypersurface, the Hamiltonian expressed in terms of the new coordinates is a function of the action variables only, $H(q_1, q_2, p_1, p_2) = H(J_1, J_2)$. The associated canonical equations, $\dot{J}_i = -\partial H/\partial \phi_i = 0$, and $\dot{\phi}_i = \partial H/\partial J_i = \omega_i(J_1, J_2)$, have trivial solutions and the phase point winds around the torus with period $2\pi/\omega_1$ the long way and with period $2\pi/\omega_2$ the short way.

If for a given torus the ratio ω_2/ω_1 is a rational number, any trajectory will close on itself. If not, the trajectory will wind around the torus and eventually cover it. The motion of the phase point (in the original coordinates as well as in the action-angle ones) is called *periodic* or *quasiperiodic* according to whether the two fundamental frequencies are *commensurate* or *incommensurate*. Hence, the existence of the analytic invariant I in addition to H imposes severe constraints not only on the course of individual trajectories in phase space but also on the motion in time of any dynamical variable.

The absence of I literally opens the gates to chaotic motion. The trajectories are no longer necessarily confined to $2d$ surfaces in phase space, and they may be able to take a much more complex course on the $3d$ energy hypersurface without violating the nonintersection requirement. Likewise, the nonexistence of action-angle coordinates removes the constraint of periodicity or quasi-periodicity and allows for more complex motion in time, characterized by continuous intensity spectra. All these new possibilities of complexity are realized by the chaotic trajectories in nonintegrable Hamiltonian systems.

We illustrate these phenomena with two examples of nonlinear Hamiltonian dynamics for systems with two degrees of freedom. Our emphasis will be on the visualization of the geometrical properties discussed previously by use of computer generated phase-space trajectories.

Our first example is the compound plane pendulum or double pendulum consisting of two equal point masses m , one suspended from a fixed support by a rigid weightless rod of length L and second suspended from the first by

a similar rod (see Fig. 1). The total energy is conserved. Is there a second independent integral of the motion? Nobody has ever found one. That is, of course, not a proof that the system is nonintegrable. However, we shall find that not all phase-space trajectories are confined to invariant tori, which demonstrates nonintegrability beyond any reasonable doubt.

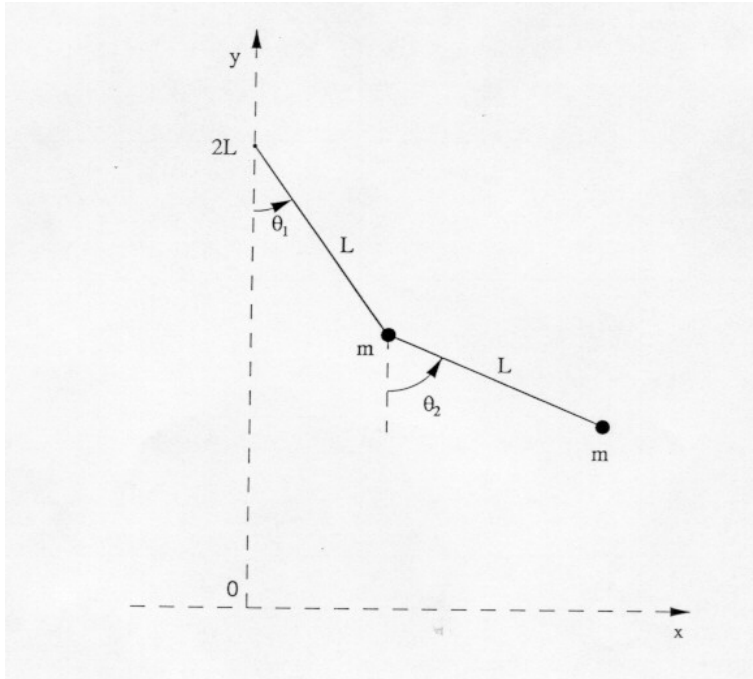


Figure 1: The double pendulum. We use units such that $m = 1$, $L = 1$, and $g = 1$.

In order to accomplish this task, we first have to find a set of canonical coordinates for the system. The general recipe for the construction of the Hamiltonian for a mechanical system can be found in textbooks on classical mechanics.³ For the double pendulum the main steps of this procedure are summarized as follows. The four Cartesian coordinates (x_1, y_1, x_2, y_2) of the two masses can be expressed in terms of two generalized coordinates (θ_1, θ_2) .

$$x_1 = L \sin \theta_1, \quad y_1 = 2L - L \cos \theta_1, \quad (2a)$$

$$x_2 = L \sin \theta_1 + L \sin \theta_2, \quad y_2 = 2L - L \cos \theta_1 - L \cos \theta_2. \quad (2b)$$

The Lagrangian \mathcal{L} is constructed as the kinetic energy minus the potential energy and is expressed in terms of the unconstrained coordinates and their time derivatives.

$$\mathcal{L} = \frac{1}{2}mL^2[2\dot{\theta}_1^2 + \dot{\theta}_2^2 + 2\dot{\theta}_1\dot{\theta}_2 \cos(\theta_1 - \theta_2) - mgL(3 - 2\cos \theta_1 - \cos \theta_2)]. \quad (3)$$

The canonical momenta $p_i = \partial\mathcal{L}/\partial\dot{\theta}_i$ conjugate to the coordinates $q_i = \theta_i$ are given by

$$p_1 = mL^2[2\dot{\theta}_1 + \dot{\theta}_2 \cos(\theta_1 - \theta_2)], \quad p_2 = mL^2[\dot{\theta}_2 + \dot{\theta}_1 \cos(\theta_1 - \theta_2)], \quad (4)$$

and are used to construct the Hamiltonian from \mathcal{L} via a Legendre transform $H = \sum_i p_i \dot{q}_i - \mathcal{L}$. We find that

$$H = \frac{1}{2mL^2} \frac{p_1^2 + 2p_2^2 - 2p_1 p_2 \cos(q_1 - q_2)}{1 + \sin^2(q_1 - q_2)} + mgL(3 - 2 \cos q_1 - \cos q_2). \quad (5)$$

The time evolution of the two pairs of canonical coordinates is determined by the canonical equations (1), yielding four coupled nonlinear first-order equations (see Problem 1).

It is instructive to write a short program that simulates the double pendulum and displays its motion on a computer screen. Except for small-amplitude oscillations, the motion of the two point masses is rather complex and evokes a sense of unpredictability. However, if we want to distinguish whether a particular run of the system is quasiperiodic or chaotic, we must sharpen our observational tools. Merely watching the swinging masses is not sufficient. We need to look for a torus.

How do we best visualize a $2d$ torus in $4d$ space on a flat screen? Suppose we want to visualize the torus on the (q_1, q_2) -plane. We can plot $q_1(t)$ versus $q_2(t)$ without regard to p_1 or p_2 . This projection will always be a continuous line. But we restrict the plot to only those phase points for which, say $p_2 = 0$ with $\dot{p}_2 > 0$. This produces a *Poincaré map*, the projection onto a plane of the intersection of the trajectory with the *surface of section* $p_2 = 0$. If a particular trajectory is confined to a torus, then the Poincaré map is confined to the intersection of the torus with the surface of section and is simply a line. If the trajectory is not confined to a torus, the map will not be restricted in that way. Chaotic trajectories have Poincaré maps that are *disorganized jumbles of points* in contrast to regular trajectories which yield Poincaré maps that are *lines* for irrational ω_2/ω_1 or a finite number of points for rational ω_2/ω_1 . This type of analysis is probably the most powerful technique for the detection and visualization of chaos in Hamiltonian systems with two degrees of freedom.

In Fig. 2 we show the Poincaré maps for six different trajectories of the double pendulum, all on the same energy hypersurface. The coordinates of the outer mass x_2, y_2 are shown at those times for which p_2 is zero and increasing. We use these coordinates instead of the canonical coordinates for illustration, since the former give the actual location of a real object in ordinary space. This cut will mirror the abstract phase space behavior. Of the six trajectories, five can be seen to lie on tori. The sixth trajectory is responsible for the chaotic jumble of points that covers most of the figure. At the center of the nested closed curves is a single dot. The corresponding trajectory is thus strictly periodic, returning to the same point in phase space over and over again. (A set of initial conditions very close to this orbit is $q_1 = -0.822, q_2 = 1.4335, p_1 = 1.5422, p_2 = 0.0$.) The small pair of closed curves outside the nested group arise from a single trajectory,

with successive crossings alternating between the two members. At the center of each is a single dot. These two dots represent a second strictly periodic trajectory, which repeats its phase space position after two passages through the surface of section, rather than after every single passage. Both of these periodic orbits are numerically stable, that is, most nearby initial conditions also lead to tori. Isolated unstable periodic orbits might exist also, but because they are not surrounded by regular regions they are more difficult to discover numerically.

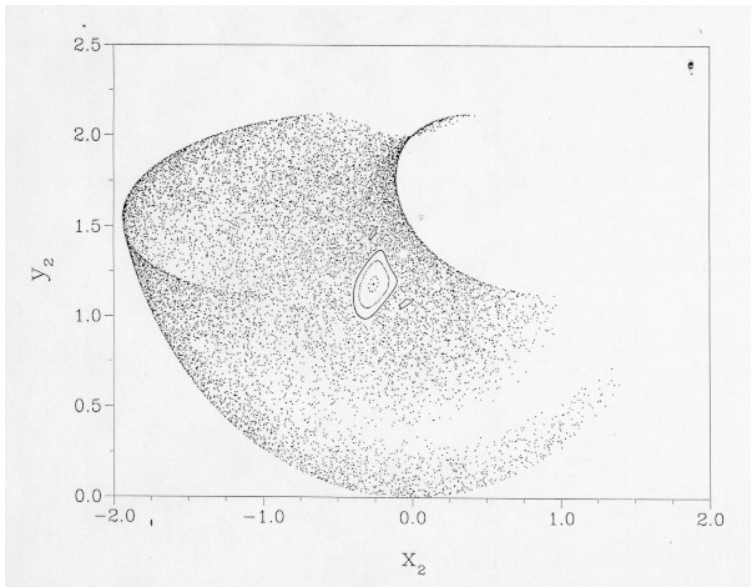


Figure 2: The Poincaré maps for five regular trajectories and one chaotic trajectory are shown for the double pendulum on the same energy hypersurface $E = E_0 = 2.24483$. The initial conditions for the regular trajectories all have $p_2 = 0$ and p_1 chosen so that $E = E_0$. For the rest of tori, starting from the outside in, the initial conditions are $q_1 = -0.65, -0.7, -0.85$ with $q_2 = 1.4$, and $(q_1 = -0.822, q_2 = 1.4335)$. The two small closed curves are both produced by the trajectory starting from $(q_1 = -0.5, q_2 = 1.4)$. The initial condition for the chaotic orbit is $(q_1 = 0.5, q_2 = \pi, p_1 = p_2 = 0)$.

Our second example differs from the usual mechanical systems, but will be useful for the study of quantum chaos that will be the subject of a future column. It is a model of two classical spins, i.e., two 3-component vectors \vec{S}_1 and \vec{S}_2 of fixed length S that are coupled one to the other. Like the double pendulum, this is a nonlinear Hamiltonian system with two degrees of freedom, but unlike the pendulum problem, which is motivated mechanically, the classical spin problem is derived from objects whose nature is intrinsically quantum mechanical.⁴ The path toward canonical variables and a phase-space description is therefore

different.

Instead of starting with the construction of a Lagrangian, we specify the system by the energy function

$$H = - \sum_{\alpha=\{x,y,z\}} \left[JS_{1\alpha}S_{2\alpha} + \frac{1}{2}A_{\alpha}(S_{1\alpha}^2 + S_{2\alpha}^2) \right] \quad (6)$$

for the six noncanonical coordinates $S_{i\alpha}$ ($i = 1, 2$), and their Poisson brackets

$$\{S_{i\alpha}, S_{j\beta}\} = -\delta_{ij} \sum_{\gamma} \epsilon_{\alpha\beta\gamma} S_{i,\gamma}, \quad (7)$$

where $\epsilon_{\alpha\beta\gamma}$ is the Levi-Civita symbol. The $S_{i\alpha}$ ($i = 1, 2$) satisfy Hamilton's equations

$$\frac{d\vec{S}_i}{dt} = \{H, \vec{S}_i\} = -\vec{S}_i \times \frac{\partial H}{\partial \vec{S}_i}. \quad (8)$$

Only four out of the six first-order differential equations in (8) are independent.

Choosing a set of canonical coordinates is equivalent to expressing $S_{i\alpha}$ in terms of two pairs of variables p_i, q_i whose Poisson brackets satisfy the conditions, $\{p_i, p_j\} = \{q_i, q_j\} = 0$ and $\{p_i, q_j\} = \delta_{ij}$. If the spin components are expressed in terms of spherical coordinates in the usual way

$$\vec{S}_i = S(\sin \theta_i \cos \phi_i, \sin \theta_i \sin \phi_i, \cos \theta_i) \quad (9)$$

then the variables ($p_i = S \cos \theta_i, q_i = \phi_i$) are indeed canonical. The canonical equations for the spin problem are then obtained by expressing (6) in terms of p_i and q_i and then using (1).

Note that the energy function (6) of the classical two-spin system does not have the form, kinetic energy plus potential energy, and that the canonical momenta have nothing in common with mass times velocity. We have left these associations completely behind.

The classical two-spin problem is completely integrable if there exists an independent integral of the motion in addition to H . We have determined that if the condition

$$(A_x - A_y)(A_y - A_z)(A_z - A_x) + J_x^2(A_y - A_z) + J_y^2(A_z - A_x) + J_z^2(A_x - A_y) = 0 \quad (9)$$

is satisfied, the system is integrable; otherwise it is nonintegrable.⁴ If we choose the parameters $J_x = J_y = 1, J_z = 0, A_x = -A_y = -1, A_z = 0$, the integrability condition (10) is satisfied. In this case we have been able to construct a second integral of the motion explicitly.⁴ We have simulated a number of different initial conditions, all on the same energy hypersurface, for this choice of the parameters and have plotted the results in Fig. 3. We show Poincaré maps of the intersections of the trajectory with the plane $\theta_2 = \pi/2$, projected onto the (q_1, p_1) plane. Unlike the case of the double pendulum, we find only lines and no jumbles illustrating the fact that in this integrable model the entire energy hypersurface is densely foliated by doughnuts.

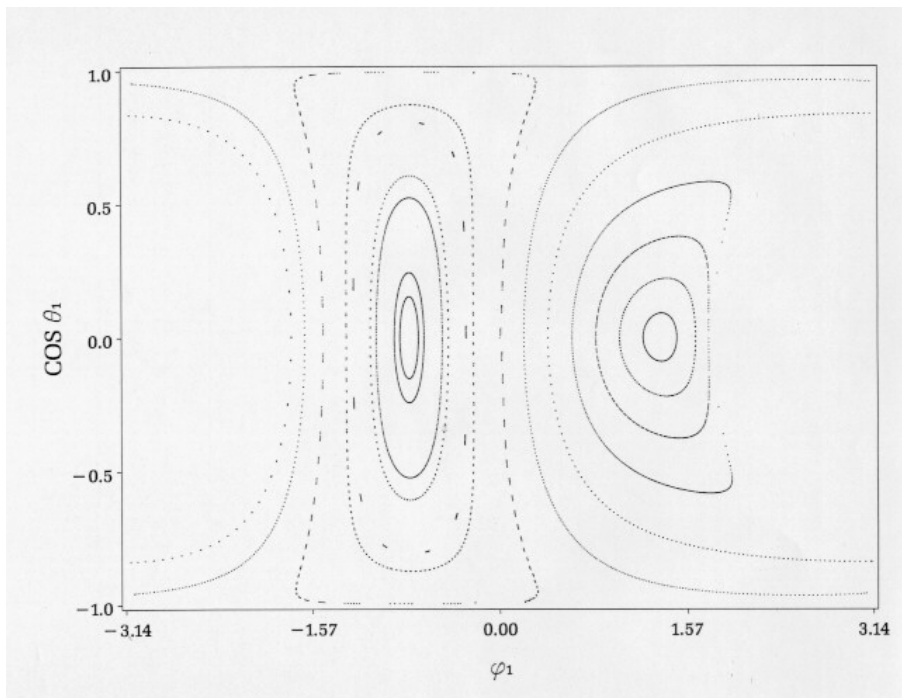


Figure 3: Poincaré maps of several phase-space trajectories for the nonlinear integrable two-spin model with $S = 1$, $J_x = J_y = 1$, $J_z = 0$, $A_x = -A_y = -1$, $A_z = 0$ and energy $E = E_0 = -0.09957501$. The cut plane is defined by $\theta_2 = \pi/2$. The initial conditions are $\theta_1 = \theta_2 = \pi/2$, $\phi_1 = -\pi + 0.2n$, where $n = 0, 1, \dots, 6$ and $n = 25, 26, \dots, 30$ and p_2 chosen in each case so that $E = E_0$.

If we choose the parameters $J_x = J_y = 1$, $J_z = 0$, $A_x = 2$, $A_y = -1$, $A_z = 0$, the integrability condition (10) is not satisfied, a second integral of the motion does not exist, and the system is nonintegrable. The time evolution is chaotic, but not necessarily for all initial conditions. Some tori do persist, but it is not easy to recognize them unless a plot of the Poincaré map is made (see Fig. 4). The top panels show two projected trajectories and the bottom two show the corresponding Poincaré maps (defined by $\theta_2 = \pi/2$). The trajectories are given for $0 < Jt < 50$, the maps over much longer times. A study of the trajectories reveals very little of the nature of the underlying motion. The two trajectories are almost indistinguishable and it is not apparent whether either trajectory is confined to a torus. However from the Poincaré maps it is obvious which is confined and which is free to wander the energy hypersurface. It is equally clear why the word chaos is used!

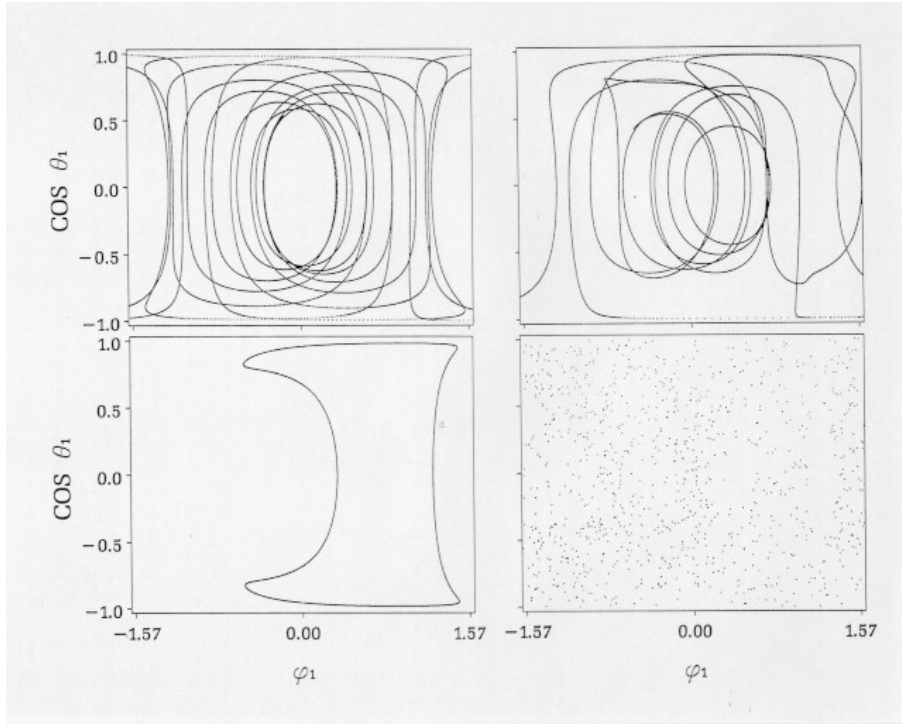


Figure 4: Two phase-space trajectories and Poincaré maps of the nonintegrable two-spin model (6) with $J_x = J_y = 1$, $J_z = 0$, $A_x = 2$, $A_y = -1$, $A_z = 0$. The initial conditions for the regular and chaotic trajectory are $(\theta_1 = 1.0, \theta_2 = 2.0, \phi_1 = 3.0, \phi_2 = 1.26)$ and $(\theta_1 = 1.0, \theta_2 = 2.0, \phi_1 = 3.0, \phi_2 = 1.29)$ respectively. The top panels show projections of the full trajectory over a short time interval and the bottom panels show projections of the Poincaré maps (surface of section $\theta_2 = \pi/2$) of the same trajectories.

Problems for further study

1. Write a program that performs an animation of the swinging double pendulum. How is the energy measured in terms of L , m , and g ? For simplicity choose dimensionless units such that L , m , and g are unity. Derive the equations of motion for the canonical variables using (5) and (1). Use the result that

$$\dot{q}_1 = \frac{p_1 - p_2 \cos(q_1 - q_2)}{mL^2[1 + \sin^2(q_1 - q_2)]} \quad (10)$$

to check your results. We have used the fourth-order Runge-Kutta algorithm⁵ to integrate the equations of motion for $\dot{q}_1, \dot{q}_2, \dot{p}_1, \dot{p}_2$. A choice of time step $\Delta t = 0.01$ should be sufficient. Note that the swinging rods will appear to shrink and stretch as their orientation changes, due to different horizontal

and vertical screen resolution and pixel size, unless special care is taken to correct for the aspect ratio.

2. Modify your program in the following way so that it draws a Poincaré map. After an integration time step, compare the value of p_2 to its previous value. If p_2 has passed through 0, plot a point on the (x_2, y_2) plane (see discussion in text). It would be desirable to draw the pendulum and the map side by side so that you can see the correspondence between the motion of the pendulum and the appearance of points on the Poincaré map.
3. (a) Find the period of the orbit at the center of the nested set of tori (see Fig. 2). (b) Find a set of initial conditions for which the Poincaré map is the pair of dots at the center of the outlying closed loops. Hint: Begin with the initial conditions $q_2 = 1.4, q_1 = -0.5, p_2 = 0$ given in Fig. 2 and modify them slightly to seek smaller loops. (c) Find the period of this trajectory.
4. Derive the equation of motion for each component of each spin for the two-spin Hamiltonian (6). Show algebraically that H is conserved. Adapt your program to draw \vec{S}_1 and \vec{S}_2 . It is possible to draw both the azimuthal and the polar motions.
5. The Poincaré map is not the only numerical technique that can be used to detect chaos. The rate of divergence of nearby trajectories is linear or exponential for regular and chaotic motion respectively. (See for example, the discussion of Lyapunov exponents in Ref. 1.) Compute the Lyapunov spectrum of the integrable and nonintegrable two-spin model and the double pendulum for trajectories in the regular and chaotic regime. Is your interpretation of the spectrum consistent with your interpretation of the Poincaré map? It is also interesting to compute the time-displaced auto-correlation functions such as $C_{1x}(t) = \langle S_{1x}(t)S_{1x}(0) \rangle$. (See Ref. 6 for a discussion of the computation of time-displaced correlation functions.) Determine if there is a qualitative difference in the behavior of $C_{1x}(t)$ for the two-spin model in the integrable and chaotic regimes.⁷
6. Consider a single spin problem defined by

$$H = \frac{1}{2}A_z S_z^2 - \gamma \vec{S} \cdot \vec{B}, \quad (11)$$

where γ and A_z are constants and B is an external magnetic field. (a) Show that the system is integrable if B is independent of time. (b) Find Hamilton's equations of motion when B depends on t . (c) Numerically integrate the equations for the two cases $B = (B \cos \omega t, 0, 0)$ and $B = (B \cos \omega t, B \sin \omega t, 0)$. Choose $A_z, B,$ and γ order unity, and integrate for many periods of the oscillating field. What can you conclude about the integrability of the system from the Poincaré maps for these two cases? (d) Prove your conclusions algebraically. See Refs. 4 and 8 for details.

We thank Harvey Gould and Jan Tobochnik for helpful suggestions. A True BASIC program for the double pendulum is available from them. Please address comments, suggestions for future columns, and requests to hgould@clarku or tobochnik%hey1.kzoo.edu.

References

1. J. Tobochnik and H. Gould, *Computers in Physics* **3**, No. 6, 86 (1989).
2. M. Tabor, *Chaos and Integrability in Nonlinear Dynamics*, Wiley, New York (1989).
3. See for example, H. Goldstein, *Classical Mechanics*, Addison-Wesley, Reading (1980) (graduate text); I. Percival and D. Richards, *Introduction to Dynamics*, Cambridge University Press (1982) (undergraduate text).
4. E. Magyari, H. Thomas, R. Weber, C. Kaufman and G. Müller, *Z. Phys. B* **65**, 363 (1987).
5. See for example, W. H. Press, B. P. Flannery, S. A. Teukolsky, and W. T. Vetterling, *Numerical Recipes*, Cambridge University Press (1986).
6. H. Gould and J. Tobochnik, *Computers in Physics* **3**, No. 4, 82 (1989).
7. N. Srivastava, C. Kaufman and G. Müller, *J. Appl. Phys.* **63**, 4154 (1988); *ibid. J. Physique C***8**, 1601 (1988).
8. H. Frahm and H. J. Mikeska, *Z. Phys. B* **60**, 117 (1985).